Limitation of phosphate assimilation maintains cytoplasmic magnesium homeostasis

Roberto E. Bruna[a], Christopher G. Kendra[a], Eduardo A. Groisman[b,c], and Mauricio H. Pontes[a,d,1]

[a]Department of Pathology and Laboratory Medicine, Pennsylvania State College of Medicine, Hershey, PA 17033; [b]Department of Microbial Pathogenesis, Yale School of Medicine, New Haven, CT 06536; [c]Yale Microbial Sciences Institute, West Haven, CT 06516 and [d]Department of Microbiology and Immunology, Pennsylvania State College of Medicine, Hershey, PA 17033

Edited by Caroline S. Harwood, University of Washington, Seattle, WA, and approved February 2, 2021 (received for review October 19, 2020)

Phosphorus (P) is an essential component of core biological molecules. In bacteria, P is acquired mainly as inorganic orthophosphate (Pi) and assimilated into adenosine triphosphate (ATP) in the cytoplasm. Although P is essential, excess cytosolic Pi hinders growth. We now report that bacteria limit Pi uptake to avoid disruption of Mg^{2+}-dependent processes that result, in part, from Mg^{2+} chelation by ATP. We establish that the MgtC protein inhibits uptake of the ATP precursor Pi when *Salmonella enterica* serovar Typhimurium experiences cytoplasmic Mg^{2+} starvation. This response prevents ATP accumulation and overproduction of ribosomal RNA that together ultimately hinder bacterial growth and result in loss of viability. Even when cytoplasmic Mg^{2+} is not limiting, excessive Pi uptake increases ATP synthesis, depletes free cytoplasmic Mg^{2+}, inhibits protein synthesis, and hinders growth. Our results provide a framework to understand the molecular basis for Pi toxicity. Furthermore, they suggest a regulatory logic that governs P assimilation based on its intimate connection to cytoplasmic Mg^{2+} homeostasis.

phosphate toxicity | ATP | magnesium | MgtC | *Salmonella*

As a component of a large number of biological molecules, phosphorus (P) is required for key biological functions. These include the formation of cellular boundaries, the storage and transfer of chemical energy, the integration and propagation of information in signal transduction pathways, and the storage, transmission, and expression of genetic information. Bacteria take up P mainly as inorganic phosphate (PO_4^{-3}; Pi), which is then assimilated in the cytoplasm via its incorporation into adenosine triphosphate (ATP). ATP functions as the main cellular P-carrier molecule, mediating both the transfer of Pi among biological molecules and the release of chemical energy to power energy-dependent processes (1). Cells must tightly regulate Pi acquisition and utilization because P assimilation is essential but excessive cytoplasmic Pi is toxic (2–9). Here, we elucidate how bacteria coordinate Pi acquisition and consumption to prevent the deleterious effects of unbalanced Pi metabolism.

Following assimilation, the negative charges from Pi groups in biomolecules are neutralized by positively charged ionic species present in the cytoplasm. As such, the majority of cytoplasmic ATP exists as a salt with positively charged magnesium (Mg^{2+}), the most abundant divalent cation in living cells. Therefore, the ATP:Mg^{2+} salt, rather than the ATP anion, is the substrate for most ATP-dependent enzymatic reactions (10, 11). In enteric bacteria, ATP stimulates transcription of ribosomal RNA (rRNA) genes (12, 13). The synthesis and activity of ribosomes consume the majority of the ATP in rapidly growing cells (14). During ribosome biogenesis, the negative charges from Pi groups in the rRNA backbone chelate large amounts of Mg^{2+} ions (14, 15). This process reduces electrostatic repulsion among Pi groups in the rRNA backbone, enabling the folding and assembly of functional ribosomes (15, 16). Thus, ATP and rRNA constitute the largest cytoplasmic reservoirs of Pi and Mg^{2+} (12, 14–20). Given this inherent connection between Pi and Mg^{2+}, we wondered if the cytotoxic effects of excessive Pi uptake result from Pi assimilation into ATP and subsequent disruption of Mg^{2+} dependent processes.

In the gram-negative bacterium *Salmonella enterica* serovar Typhimurium (*Salmonella*), prolonged growth in limiting Mg^{2+} induces a Mg^{2+} starvation response mediated by the MgtA, MgtB and MgtC proteins (21–24). MgtA and MgtB are high-affinity, ATP-dependent Mg^{2+} importers that increase the Mg^{2+} concentration in the cytoplasm (25, 26). MgtC decreases intracellular ATP levels (27), thereby reducing rRNA synthesis, which lowers the steady-state amounts of ribosomes and slows down the translation rate (28). This response reduces the concentration of assimilated P and, consequently, the quantity of Mg^{2+} required as a counter ion, allowing the remaining cytoplasmic Mg^{2+} to stabilize existing ribosomes and to maintain other vital cellular processes that exhibit a strict dependence on Mg^{2+} (21, 28, 29).

MgtC promotes *Salmonella* survival inside mammalian macrophages and the establishment of systemic infections (30, 31). In macrophages, MgtC inhibits the activity of *Salmonella*'s own F_1F_o ATP synthase, the enzyme catalyzing ATP production via oxidative phosphorylation (32, 33). MgtC appears to operate by distinct mechanisms inside macrophages versus low-Mg^{2+} media because an MgtC variant has been identified that fails to promote intramacrophage survival while enabling growth and viability under cytoplasmic Mg^{2+} starvation (34). In this paper, we reveal that Pi uptake must be tightly controlled to maintain cytoplasmic Mg^{2+} homeostasis. We establish that during cytoplasmic Mg^{2+} starvation, MgtC lowers ATP levels by inhibiting Pi uptake,

Significance

Phosphorus (P) is essential for life. As the fifth-most-abundant element in living cells, P is required for the synthesis of an array of biological molecules including (d)NTPs, nucleic acids, and membranes. Organisms typically acquire environmental P as inorganic phosphate (Pi). While essential for growth and viability, excess intracellular Pi is toxic for both bacteria and eukaryotes. Using the bacterium *Salmonella enterica* serovar Typhimurium as a model, we establish that Pi cytotoxicity is manifested following its assimilation into adenosine triphosphate (ATP), which acts as a chelating agent for Mg^{2+} and other cations. Our findings identify physiological processes disrupted by excessive Pi and how bacteria tune P assimilation to cytoplasmic Mg^{2+} levels.

Author contributions: R.E.B., C.G.K., E.A.G., and M.H.P. designed research; R.E.B., C.G.K., and M.H.P. performed research; E.A.G. and M.H.P. contributed new reagents/analytic tools; R.E.B., C.G.K., and M.H.P. analyzed data; and R.E.B. and M.H.P. wrote the paper.

The authors declare no competing interest.

This article is a PNAS Direct Submission.

This open access article is distributed under Creative Commons Attribution-NonCommercial-NoDerivatives License 4.0 (CC BY-NC-ND).

[1]To whom correspondence may be addressed. Email: mpontes@pennstatehealth.psu.edu.

This article contains supporting information online at https://www.pnas.org/lookup/suppl/doi:10.1073/pnas.2021370118/-/DCSupplemental.

Published March 11, 2021.

MICROBIOLOGY

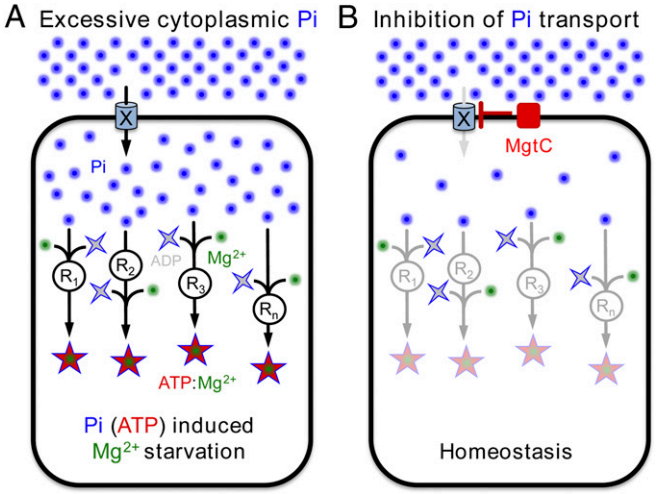

Fig. 1. Model depicting how *Salmonella enterica* prevents Pi cytotoxicity. (*A*) Excessive Pi is imported into the cytoplasm via an inner membrane transport system (denoted by an X). Pi is assimilated by the cells through reactions that synthesize ATP (R_1, R_2, R_3, R_n). Excessive ATP chelates free cytoplasmic Mg^{2+}, thereby inducing cytoplasmic Mg^{2+} starvation. (*B*) Cells express the MgtC membrane protein to inhibit Pi uptake via X. The reduction in the availability of cytoplasmic Pi simultaneously slows all ATP-generating reactions in the cell, freeing Mg^{2+} ions and restoring homeostasis.

thus limiting an ATP precursor instead of interfering with its enzymatic generation (Fig. 1). MgtC hinders the activity of the main Pi uptake system in *Salmonella* and likely other bacterial species. Counterintuitively, limiting exogenous Pi availability rescues translation, promotes growth, and restores viability to an *mgtC* null mutant. Excess Pi is toxic even at physiological concentrations of cytoplasmic Mg^{2+} due to its incorporation into ATP and subsequent disruption of Mg^{2+}-dependent processes. Our findings provide a conceptual framework to understand the underlying basis of Pi cytotoxicity observed in bacteria and eukaryotes (3–9, 35–38). Moreover, we uncover the regulatory logic by which cells control of P assimilation.

Results

The MgtC Protein Limits ATP Accumulation during Low Cytoplasmic Mg^{2+} Stress by an F_1F_o Synthase-Independent Mechanism. ATP exists as a Mg^{2+} salt in living cells (11, 14). Therefore, when cells face limiting cytoplasmic Mg^{2+} concentrations, they reduce ATP amounts to free Mg^{2+} ions so they can be used for other cellular processes, such as ribosome assembly (28, 29). In macrophages, MgtC inhibits *Salmonella*'s own F_1F_o ATP synthase, the enzyme responsible for ATP synthesis via oxidative phosphorylation (32). Notably, an *mgtC atpB* double mutant—lacking both MgtC and the AtpB subunit of the ATP synthase—was reported to harbor similar ATP amounts than an *atpB* single mutant under cytoplasmic Mg^{2+} starvation conditions (32). This result led to the notion that MgtC prevents a nonphysiological rise in ATP levels by inhibiting the F_1F_o ATP synthase also under cytoplasmic Mg^{2+} starvation (32, 39, 40). Below, we present the result of experiments that reexamine the interpretation of the aforementioned results.

The F_1F_o ATP synthase uses the proton motive force generated by the respiratory electron transport chain to synthesize ATP from adenosine diphosphate and Pi (41, 42). Consequently, an *mgtC atpB* double mutant (or any other strain lacking a functional ATP synthase) relies exclusively on fermentative pathways to produce ATP via substrate-level phosphorylation (43). However, the low ATP amounts observed in the *mgtC atpB* double mutant were obtained during growth on medium containing glycerol as the carbon source (32). Given that the glycerol fermentation is extremely inefficient (44, 45), we reasoned that the low ATP amounts in the *mgtC atpB* double mutant could simply reflect an inability to efficiently ferment glycerol.

To test this notion, we compared ATP amounts in wild-type, *mgtC*, *atpB*, and *mgtC atpB* isogenic strains grown in minimal medium containing readily fermentable glucose as the carbon source and low (10 μM) Mg^{2+} to induce cytoplasmic Mg^{2+} starvation (22, 23). As hypothesized, *mgtC* and *mgtC atpB* strains had 42- and 29-fold higher ATP amounts relative to their *mgtC*$^+$ isogenic counterparts, respectively (Fig. 2*A*), after 5 h of growth, when cytoplasmic Mg^{2+} becomes limiting (28). Hence, *atpB* inactivation does not abrogate the intracellular ATP accumulation resulting from *mgtC* inactivation provided that bacteria are fed glucose as carbon source.

To further test our hypothesis, we compared ATP amounts among the four strains at 90 min following a nutritional downshift from medium containing high (10 mM) Mg^{2+} and glucose, to media lacking Mg^{2+} and containing one of various carbon sources that are metabolized via distinct pathways (Fig. 2*B*). During cytoplasmic Mg^{2+} starvation, the *mgtC* strain had higher ATP amounts than the wild-type strain regardless of the carbon source (Fig. 2*C*). By contrast, the *mgtC atpB* strain had higher ATP amounts than the *atpB* single mutant during growth on readily fermentable carbon sources (glucose, gluconate, arabinose, or pyruvate) but was unable to do so during growth on inefficiently

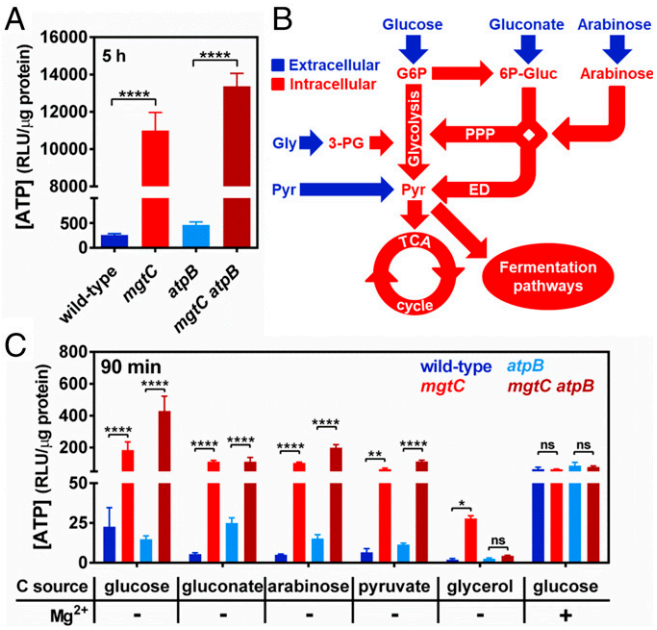

Fig. 2. F_1F_o synthase-independent ATP accumulation in an *mgtC* mutant during cytoplasmic Mg^{2+} starvation. (*A*) Intracellular ATP levels in wild-type (14028s), *mgtC* (EL4), *atpB* (MP24), or *mgtC atpB* (MP25) *Salmonella* following 5 h of growth. Cells were grown in MOPS medium containing 10 μM $MgCl_2$ and 2 mM K_2HPO_4. (*B*) Schematic representation of carbon flow through the central metabolic pathways in bacteria with key extracellular (blue) and intracellular (red) metabolites. G6P, glucose-6-phosphate; 6P-Gluc, 6-Phosphogluconate; Gly, glycerol; Pyr, pyruvate; PPP, pentose phosphate pathway; ED, Entner–Doudoroff pathway. (*C*) Intracellular ATP levels in wild-type (14028s), *mgtC* (EL4), *atpB* (MP24), or *mgtC atpB* (MP25) *Salmonella*. Cells were grown in MOPS medium containing 10 mM $MgCl_2$, 2 mM K_2HPO_4, and 25 mM glucose until OD_{600} ~0.4, washed thrice, and grown for additional 90 min in MOPS medium supplemented with the indicated carbon source (25 mM glucose, 25 mM sodium gluconate, 30 mM L-arabinose, 50 mM sodium pyruvate, or 50 mM glycerol) and containing 2 mM K_2HPO_4 and either 0 (−) or 10 (+) mM $MgCl_2$. Means ± SDs of three independent experiments are shown. $^*P < 0.05$, $^{**}P < 0.01$, $^{****}P < 0.0001$; ns, no significant difference. (*A*) Two-tailed *t* test; (*C*) two-way ANOVA with Tukey's correction.

fermentable glycerol (Fig. 2 *B* and *C*). As a control, all the strains tested displayed similar ATP amounts when resuspended in high Mg^{2+} glucose-containing medium (Fig. 2*C*). Taken together, these results indicate that the low ATP levels previously observed in an *mgtC atpB* strain experiencing cytoplasmic Mg^{2+} starvation (32) are caused by an inability to efficiently ferment glycerol as opposed to an inability to inhibit the F_1F_o ATP synthase. Furthermore, these results indicate that MgtC inhibits multiple ATP-generating reactions in the cell, not just the one that is carried out by the F_1F_o complex.

MgtC Inhibits Pi Acquisition Thereby Limiting ATP Synthesis during Cytoplasmic Mg^{2+} Starvation. Cellular ATP can be synthesized by several catabolic reactions (46–48). How, then, can MgtC control the activity of multiple ATP-producing enzymatic reactions? We reasoned that regardless of the identity of the enzymes catalyzing ATP formation, the overall rate of ATP synthesis in the cell could be restricted by the availability of substrates. MgtC could, therefore, function by inhibiting the synthesis or acquisition of an ATP precursor. Interestingly, at the onset of cytoplasmic Mg^{2+} starvation, a temporary shortage in the concentration of free cytoplasmic Mg^{2+} destabilizes the bacterial ribosomal subunits (28). The resulting decrease in translation efficiency reduces ATP consumption and, consequently, the recycling of Pi from ATP. This lowers the concentration of cytoplasmic Pi, transiently activating the cytoplasmic Pi-starvation sensing two-component system composed of the PhoB and PhoR proteins (PhoB/PhoR) (17). Three lines of evidence led us to hypothesize that MgtC prevents ATP synthesis by limiting Pi influx into the cell. First, PhoB/PhoR activation is hampered in an *mgtC* mutant (17), indicating that this strain experiences excess cytoplasmic Pi. Second, *mgtC* and *mgtC atpB* strains have higher intracellular steady-state Pi amounts than wild-type and *atpB Salmonella* strains (Fig. 3*A*), respectively. Thus, MgtC prevents Pi accumulation in an *atpB*-independent fashion. And third, when Mg^{2+} and Pi are abundant, heterologous expression of the *mgtC* gene activates PhoB/PhoR, further suggesting that MgtC causes a shortage in cytoplasmic Pi (*SI Appendix*, Fig. S1) (17).

To test our hypothesis, we measured transport of radiolabeled Pi (^{32}Pi) following MgtC expression from its native chromosomal location in response to cytoplasmic Mg^{2+} starvation. We established that *mgtC* cells accumulated four times more radioactivity than the isogenic wild-type strain after 30 min of growth in the presence of ^{32}Pi (Fig. 3*B*). This result suggests that the increased steady-state intracellular Pi levels observed for *mgtC* and *mgtC atpB* mutants (Fig. 3*A*) arises from increased uptake of extracellular Pi rather than to increased Pi release from intracellular sources. Note that all ^{32}Pi transport assays were performed in the presence of cold Pi, at a molar ratio of 1:25 (^{32}Pi:Pi), to prevent expression of the PstSCAB Pi transporter resulting from a lack of Pi in the growth medium (1). Therefore, this assay underestimates Pi influx into cells (see *Discussion* and *Materials and Methods*).

If MgtC restricts Pi import to the cytoplasm and Pi is required for ATP synthesis, a decrease in Pi availability in the growth medium should correct the high ATP amounts of the *mgtC* mutant. To test this prediction, we measured ATP amounts in wild-type and *mgtC* cells grown in minimal media with low Mg^{2+} and decreasing concentrations of exogenous Pi. Note that bacteria are able to grow in medium lacking exogenous Pi due to the residual Pi present in the mixture of casamino acids supplemented to the culture medium (see *Materials and Methods*). Strikingly, a decrease in exogenous Pi from 500 to 0 μM lowered ATP amounts in the *mgtC* mutant to wild-type levels (Fig. 3*C*). By contrast, ATP amounts remained invariably low in the wild-type strain (Fig. 3*C*). Importantly, in the absence of exogenous Pi, wild-type and *mgtC* strains had similar ATP amounts (Fig. 3*C*). Taken together, these results indicate that MgtC controls ATP synthesis by limiting Pi uptake.

MgtC Inhibits a Noncanonical Pi Transport System. *Salmonella* encodes two bona fide Pi import systems: *pitA* and *pstSCAB* (Fig. 4*A*). While PitA functions as a metal:phosphate (M:Pi)/proton symporter (1, 49–51), PstSCAB is a high affinity, ATP-dependent Pi transporter (Fig. 4*A*) (1, 8, 51, 52). In addition to *pitA* and *pstSCAB*, *Salmonella* also harbors an *yjbB* homolog, which encodes a sodium/phosphate symporter. Whereas YjbB promotes Pi export (53), we made the cautious assumption that YjbB may also import Pi (Fig. 4*A*).

To test MgtC's role on inhibition of PitA, PstSCAB, or YjbB, we measured ^{32}Pi uptake following ectopic MgtC expression in wild-type and isogenic *pitA pstSCAB yjbB* triple mutant (3ΔPi) *Salmonella*. ^{32}Pi uptake was slightly (17%) lower in wild-type *Salmonella* expressing MgtC than in those with the vector control (Fig. 4*B*). By contrast, MgtC reduced Pi uptake by 70% in the 3ΔPi background relative to the vector control (Fig. 4*B*). Because MgtC decreases Pi influx in a *pitA*-, *pstSCAB*-, and *yjbB*-independent manner, we reasoned that there must be an additional Pi influx system. In support of this notion, the 3ΔPi mutant

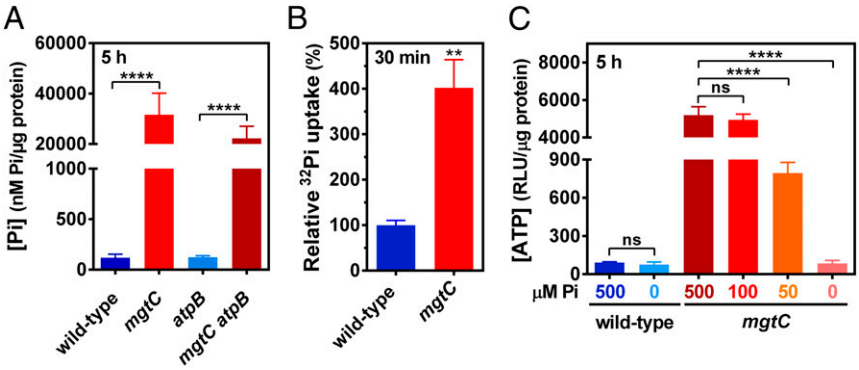

Fig. 3. MgtC-dependent inhibition of Pi transport and assimilation into ATP during cytoplasmic Mg^{2+} starvation. (*A*) Total intracellular Pi in wild-type (14028s), *mgtC* (EL4), *atpB* (MP24), or *mgtC atpB* (MP25) *Salmonella* following 5 h of growth in MOPS medium containing 10 μM $MgCl_2$ and 2 mM K_2HPO_4. (*B*) Relative radioactive orthophosphate (^{32}Pi) uptake in wild-type (14028s) or *mgtC* (EL4) cells. Bacteria were grown in MOPS medium containing 10 μM $MgCl_2$ and 500 μM K_2HPO_4 during 3 h before the addition of ^{32}Pi to the cultures. Levels of ^{32}Pi accumulated in cells were determined after 30 min of labeling by liquid scintillation counting, as described in *Materials and Methods*. ^{32}Pi uptake values were normalized against the wild-type strain. (*C*) Intracellular ATP levels in wild-type (14028s) or *mgtC* (EL4) *Salmonella* following 5 h of growth in MOPS medium containing 10 μM $MgCl_2$ and the indicated concentration of K_2HPO_4 (μM Pi). Means ± SDs of at least three independent experiments are shown. $^{**}P < 0.01$, $^{****}P < 0.0001$; ns, no significant difference. (*A*–*C*) Two-tailed *t* tests.

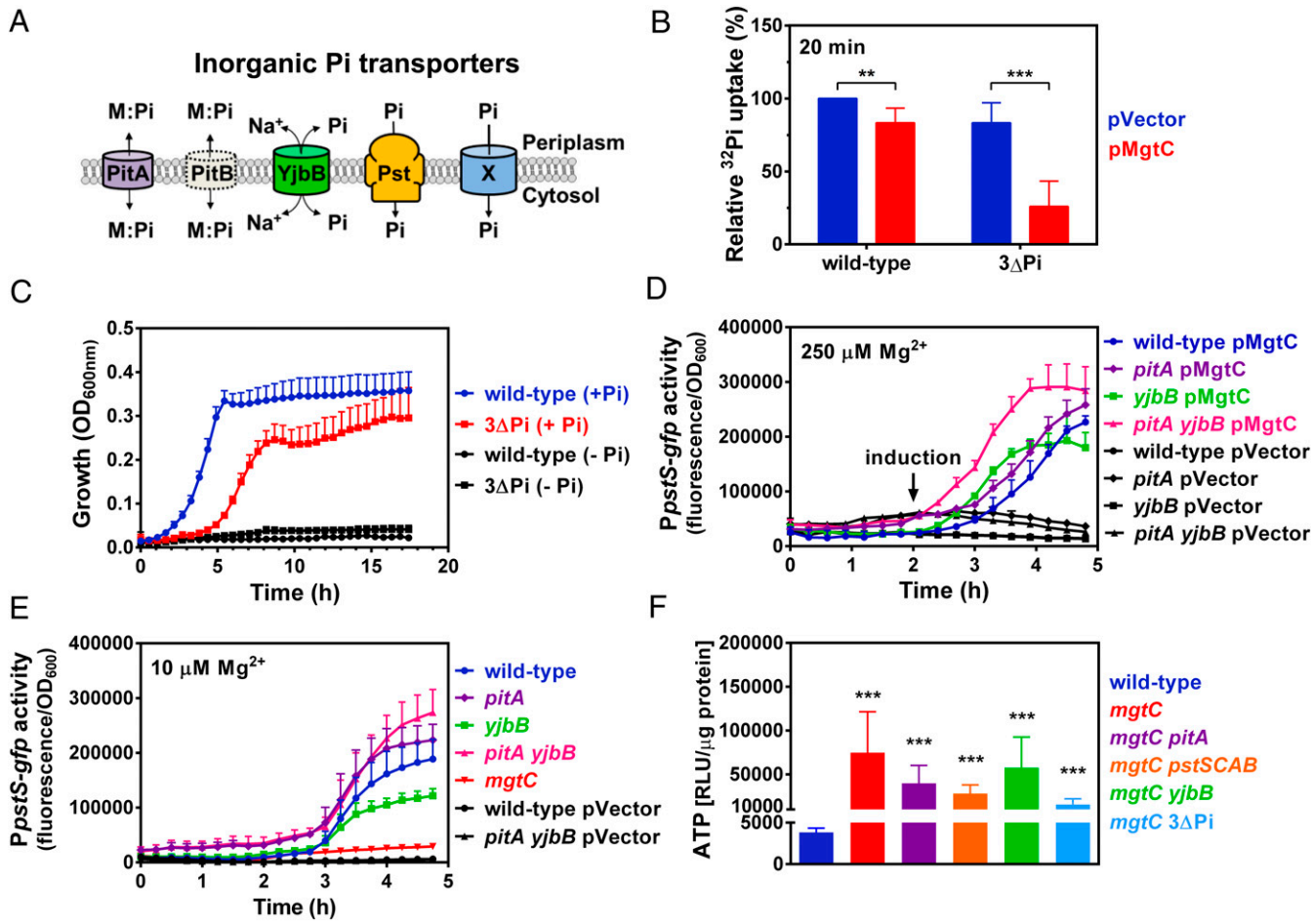

Fig. 4. A noncanonical Pi transport system is inhibited by MgtC. (*A*) Schematic representation of inorganic Pi transporters harbored by *Salmonella enterica* and *Escherichia coli*. Note that PitB (gray, dashed outline) is absent from *Salmonella*. M:Pi, metal-phosphate complex; X, inferred, uncharacterized Pi transporter inhibited by MgtC. (*B*) Relative ^{32}Pi uptake in wild-type (14028s) or Δ3Pi (RB39) carrying either pVector (pUHE-21) or pMgtC (pUHE-MgtC). Bacteria were grown in MOPS medium containing 250 μM $MgCl_2$ and 500 μM K_2HPO_4 until OD_{600} ~0.2. Cultures were then propagated for 15 min in the presence of 750 μM IPTG prior to the addition of ^{32}Pi. Transport of ^{32}Pi was allowed to take place for 20 min. Intracellular ^{32}Pi accumulation was determined by liquid scintillation counting, as described in *Materials and Methods*. ^{32}Pi uptake values were normalized against the wild-type pVector strain. $^{**}P < 0.01$, $^{***}P < 0.001$, unpaired two-tailed *t* test. (*C*) Growth curve of wild-type (14028s) or Δ3Pi (RB39) *Salmonella*. Cells were grown in MOPS medium containing 10 mM $MgCl_2$ and either 0 (−Pi) or 500 (+Pi) μM of K_2HPO_4. (*D*) Fluorescence from wild-type (14028s), *pitA* (MP1251), *yjbB* (MP1252), and *pitA yjbB* (MP1479p) *Salmonella* carrying pP*pstS*-GFPc and either pVector or pMgtC. Cells were grown in MOPS medium containing 250 μM $MgCl_2$ and 500 μM K_2HPO_4. A total of 250 μM of IPTG were added after 2 h of growth. (*E*) Fluorescence from wild-type (14028s), *pitA* (MP1251), *yjbB* (MP1252), *pitA yjbB* (MP1479p), and *mgtC* (EL4) *Salmonella* carrying pP*pstS*-GFPc or pVector (the promoterless GFP plasmid pGFPc). Cells were grown in MOPS medium containing 10 μM $MgCl_2$ and 500 μM K_2HPO_4. (*F*) Intracellular ATP levels in wild-type (14028s), *mgtC* (EL4), *mgtC pitA* (MP1254), *mgtC pstSCAB* (MP1720), *mgtC yjbB* (MP1255), or *mgtC* Δ3Pi (RB43) *Salmonella*. Cells were grown in MOPS medium containing 10 mM Mg and 2 mM 2-AP OD_{600} ~0.4. Cells were subsequently washed thrice with MOPS medium lacking $MgCl_2$ and any P source and grown for additional 90 min in MOPS medium lacking Mg^{2+} and containing 2 mM K_2HPO_4. $^{***}P < 0.001$, unpaired two-tailed *t* tests against the wild-type strain. For all graphs (*B*–*F*), means ± SDs of at least three independent experiments are shown.

grew using Pi as the sole P source (Fig. 4*C*), albeit with a longer lag and to a lower final optical density unit (OD_{600}) than the wild-type strain (Fig. 4*C*).

Two additional lines of evidence indicate that MgtC inhibits a noncanonical Pi transporter. First, by decreasing cytoplasmic Pi amounts (Figs. 3 and 4*B*), heterologous MgtC expression elicits a dose-dependent activation of PhoB/PhoR that results in transcription of the PhoB-activated *pstSCAB* operon (*SI Appendix*, Fig. S1) (17). Hence, removal of the Pi transporter targeted by MgtC should result in MgtC-irresponsive constitutively high *pstS* expression because MgtC would no longer impact PhoB/PhoR activation. We determined that MgtC expression (either heterologously in medium containing 250 μM Mg^{2+} or natively in medium containing 10 μM Mg^{2+}) induced *pstS* transcription in *pitA*, *yjbB*, and *pitA yjbB* mutants (Fig. 4 *D* and *E*). We did not examine the *pstSCAB* mutant because the PstSCAB transporter participates in the regulation of the PhoB/PhoR two-component system through a physical interaction (54). Consequently, inactivation of the transporter through mutations in *pst* genes leads to PhoB/PhoR hyperactivation, effectively preventing signal transduction (1, 3, 54, 55). In addition, we reasoned that it would be highly unlikely for cells to harbor a regulatory circuit whereby MgtC inhibition of PstSCAB transporter activity would promote PstSCAB expression (*SI Appendix*, Fig. S1) (17), requiring more MgtC protein, ad infinitum.

And second, deleting the MgtC-inhibited Pi transporter should correct the exacerbated ATP accumulation of the *mgtC* mutant (Fig. 3*C*). However, mutations in either *pitA*, *pstSCAB*, or *yjbB* or a combined deletion of all these genes did not lower ATP amounts in the *mgtC* mutant (Fig. 4*F*). Note that due to the longer lag time of 3ΔPi mutant strains growing with Pi as the sole P source (Fig. 4*C*), we cultured all tested strains in minimal medium containing 2-aminoethylphosphonic acid [2-AP] as the P source and

subsequently subjected them to a nutritional downshift to medium supplemented with 2 mM Pi and lacking Mg^{2+} for 90 min prior to ATP quantification. Because 2-AP is imported into the cytoplasm through an organic P system (PhnSTUV) prior to removal of Pi, this allows cells to bypass the need for inorganic P source and grow at the same rate. In sum, these results indicate that MgtC inhibits Pi uptake by targeting an unidentified Pi transporter.

Phosphate Limitation Rescues the Translation and Growth Defects of an *mgtC* Mutant Experiencing Cytoplasmic Mg^{2+} Starvation. An *mgtC* mutant experiencing cytoplasmic Mg^{2+} starvation exhibits ribosomal assembly defects, inefficient translation, growth arrest, and a loss of viability (21, 28). This is presumably due to Mg^{2+} chelation by excess ATP molecules because the *mgtC* mutant phenotypes are corrected by promoting ATP hydrolysis (28, 29). Given that MgtC lowers ATP synthesis by inhibiting Pi acquisition (Figs. 3 *A* and *C* and 4*B*), these phenotypes should also be rescued by limiting Pi access.

As predicted, wild-type and *mgtC* strains showed similar translation rates in the absence of exogenous Pi (Fig. 5 *A* and *B*). By contrast, during growth in 500 μM Pi, the translation rate of the *mgtC* mutant was 4.7-fold lower than that of the wild-type strain (Fig. 5 *A* and *B*). Moreover, decreasing exogenous Pi in the growth medium from 500 to 0 μM progressively increased growth of the *mgtC* mutant (Fig. 5*C*). Remarkably, in the absence of exogenous Pi, the *mgtC* mutant displayed growth yield and kinetics indistinguishable from that of the wild-type strain (Fig. 5*C*). As expected, growth of wild-type and *mgtC* strains was indistinguishable in medium containing 500 μM Pi when the Mg^{2+} concentration was raised from 10 to 500 μM (Fig. 5*C*), thereby preventing Mg^{2+} starvation. Furthermore, the loss of viability of the *mgtC* mutant (21) in medium containing 500 μM Pi was suppressed by not adding Pi (Fig. 5*D*). The mutant maintained the same number of colony-forming units (CFU) per OD_{600} as the wild-type strain. Altogether, these results establish that MgtC prevents the toxic effects of excessive Pi uptake.

Excess Pi Is Toxic Even under High Mg^{2+} Conditions. Excessive Pi uptake hinders bacterial growth even when Mg^{2+} is not limiting and cells are not anticipated to experience cytoplasmic Mg^{2+} starvation (3, 9). For instance, mutations that increase PstSCAB activity or expression cause heightened Pi uptake and growth inhibition in *Escherichia coli* (1–3, 5). The data presented in the previous sections suggest that the growth inhibition resulting from PstSCAB overexpression results from excessive Pi incorporation into ATP and subsequent chelation of Mg^{2+}, that, in turn, give rise to elevated ATP levels, inhibition of translation and growth, and induction of MgtC expression (21, 27, 28). Because these phenotypes are observed during cytoplasmic Mg^{2+} starvation, they may be corrected by increasing the availability of free cytoplasmic Mg^{2+} (e.g., through the provision of excess Mg^{2+} in the growth medium) or the reversal of Pi assimilation (e.g., through enzymatic hydrolysis of ATP) (21, 28, 29).

First, we determined the phenotypic consequences of ectopic PstSCAB expression in medium containing high (10 mM) Pi and intermediate (0.1 mM) Mg^{2+} concentrations, two conditions that do not typically result in cytoplasmic Mg^{2+} starvation (22, 23) and, thus, MgtC expression (*SI Appendix*, Fig. S2). We established that ATP amounts were four times higher in PstSCAB-expressing bacteria than in control strains harboring either an empty vector or a plasmid expressing the inner membrane protein PmrB (Fig. 6*A*). Notably, the PstSCAB-dependent increase in ATP amounts is accompanied by reductions in growth rate and growth yield, phenotypes not observed in the control strains (Fig. 6*B*).

And second, the growth defect resulting from PstSCAB expression is caused by an increase in ATP amounts resulting in chelation of free Mg^{2+}. This is because PstSCAB expression caused only a minor reduction in growth rate, enabling cells to reach the same growth yields as the control strains when the Mg^{2+} concentration was increased 100-fold (to 10 mM) (Fig. 6*C*). Importantly, Mg^{2+} rescued growth of the PstSCAB-expressing strain even though ATP amounts remained fourfold higher than those of the control strains harboring the empty vector or the PmrB-expressing plasmid (Fig. 6*A*). In addition, a plasmid-encoded soluble subunit of the ATPase (17) corrected the growth defect caused by PstSCAB expression (Fig. 6*D*) whereas the vector

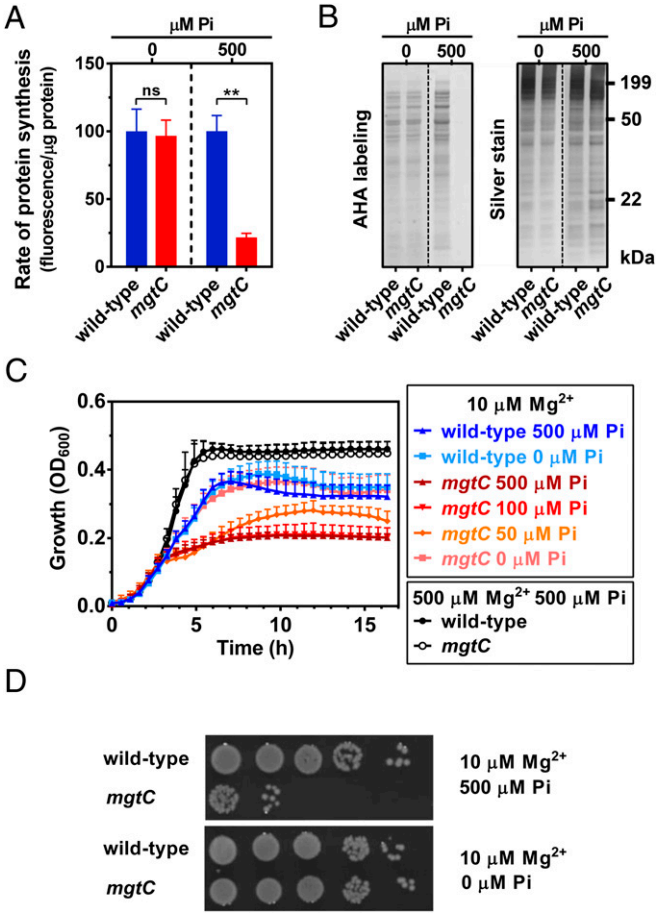

Fig. 5. Effect of phosphate limitation on the translation rate, growth, and viability of an *mgtC* mutant during cytosolic Mg^{2+} starvation. (*A*) Quantification and (*B*) Sodium dodecyl sulfate–polyacrylamide gel electrophoresis (SDS-PAGE) analysis of the rate of protein synthesis (L-azidohomoalanine [AHA] labeling) of wild-type or *mgtC* (EL4) *Salmonella.* Cells were grown in MOPS medium containing 10 mM $MgCl_2$ and 2 mM K_2HPO_4 until OD_{600} ~0.4. Cells were subsequently washed thrice with MOPS medium lacking $MgCl_2$, K_2HPO_4, and amino acids and grown for additional 90 min in MOPS medium lacking methionine and containing 10 μM $MgCl_2$ plus the indicated concentration of K_2HPO_4 (μM Pi). Means ± SDs of four independent experiments are shown. $^{**}P < 0.01$, unpaired two-tailed *t* test. ns, no significant difference. The gel is representative of four independent experiments. Samples from 0 and 500 μM Pi were resolved and imaged from different gels (indicated by dashed lines). (*C*) Growth curve of wild-type (14028s) or *mgtC* (EL4) *Salmonella*. Cells were grown in MOPS medium containing the indicated concentrations of $MgCl_2$ and K_2HPO_4. Means ± SDs of three independent experiments are shown. (*D*) Viable cell count of wild-type (14028s) or *mgtC* (EL4) *Salmonella* following 16 h of growth in MOPS medium containing 10 μM $MgCl_2$ and 0 or 500 μM K_2HPO_4. Cell suspensions were normalized to the same OD_{600} and diluted, and 5 μL was spotted on plates. Images were taken after incubation of plates at 37 °C for 18 h and are representative of three independent experiments.

MICROBIOLOGY

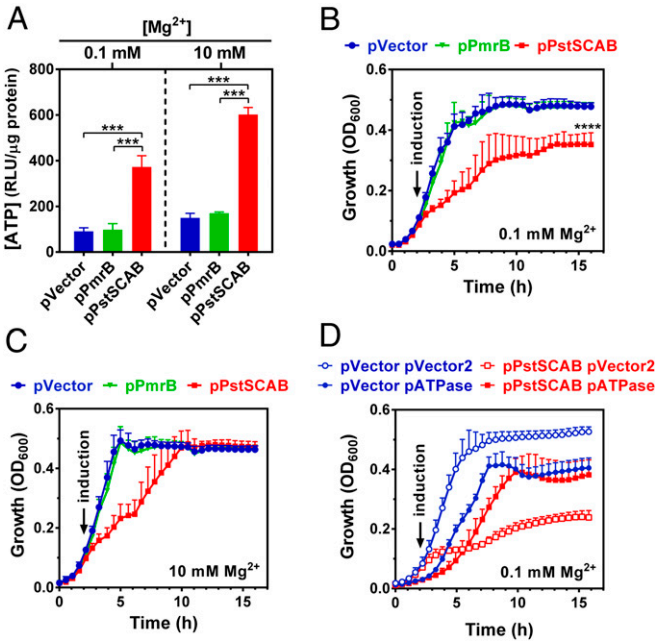

Fig. 6. Effect of PstSCAB on growth, P assimilation, and Mg^{2+} homeostasis. (*A*) Intracellular ATP levels of cultures depicted in *B* and *C*. Measurements were conducted at 5 h of growth. (*B*, *C*) Growth curves of wild-type (14028s) *Salmonella* carrying pVector (pUHE-21), pPstSCAB (pUHE-PstSCAB), or pPmrB (pUHE-PmrB) in MOPS medium containing 0.1 (*B*) and 10 mM $MgCl_2$ (*C*). (*D*) Growth curve of wild-type (14028s) *Salmonella* carrying either pVector or pPstSCAB and either pVector2 (pBbB2K-GFP) or pATPase (pBbB2K-AtpAGD). In all experiments, cells were grown in MOPS medium containing 10 mM K_2HPO_4 and the indicated $MgCl_2$ concentration. Ectopic protein expressions were induced by adding 250 μM IPTG to the cultures after 2 h of growth. Means ± SDs of three independent experiments are shown. (*A*, *B*) ***$P < 0.001$, ****$P < 0.0001$, unpaired two-tailed *t* test against pVector.

control did not (Fig. 6*D*). Taken together, these results indicate that excess Pi imported into the cytoplasm is rapidly assimilated into ATP, causing a decrease in the levels of free cytoplasmic Mg^{2+} and inhibiting growth.

Excessive Pi Uptake Impairs Translation and Promotes MgtC Expression during Growth in High Mg^{2+}. If excessive Pi uptake leads to physiological conditions resembling cytoplasmic Mg^{2+} starvation (Fig. 6 *A–D*) (21, 28, 29), then increased Pi uptake resulting from PstSCAB expression should also decrease translation rates. Furthermore, because a reduction in translation rates caused by cytoplasmic Mg^{2+} starvation promotes *mgtC* transcription (22, 23, 27, 28, 56), excessive Pi uptake should also promote MgtC expression. We tested these predictions by measuring temporal fluorescence changes in wild-type strains harboring both a plasmid-borne *gfp* transcriptional fusion to the promoter and leader regions of *mgtC*, and either the empty vector, the pPmrB plasmid, or the pPstSCAB plasmid.

Fluorescence from *mgtC-gfp* increased 1 h following PstSCAB induction (Fig. 7*A*). This increase was absent or delayed in the control strains harboring the empty vector or expressing PmrB (Fig. 7*A*). Note that during growth in 25 μM Mg^{2+}, the control strains display a minor increase in fluorescence after 4 h of growth. This small increase in fluorescence results from late onset of cytoplasmic Mg^{2+}, which is delayed when compared to cells grown at 10 μM Mg^{2+} (*SI Appendix*, Fig. S2) (17, 22, 23, 57). The effect of PstSCAB expression on the time and fluorescence levels of the *mgtC-gfp* strain was inversely related to the availability of Mg^{2+} in the growth medium. That is, fluorescence resulting from PstSCAB expression in cultures grown in 25 μM Mg^{2+} were higher than those grown in 50 μM Mg^{2+}, which, in turn, were higher than those grown in 0.1 mM Mg^{2+} (Fig. 7*A*). Bacteria grown in 0.1 mM Mg^{2+} displayed a relatively mild increase in *mgtC-gfp* activity 1 h after PstSCAB expression, and their fluorescence levels rose rapidly at 7.5 h post induction (Fig. 7*A*). The delayed *mgtC* induction likely reflects the time at which bacteria no longer neutralize the excess of intracellular Pi incorporated into ATP because they exhausted the Mg^{2+} available in the growth medium and, consequently, are unable to efficiently stabilize their ribosomes (28). We conclude that increased ATP production resulting from excessive Pi assimilation disrupts translation by sequestering free Mg^{2+} ions.

To determine whether excessive Pi uptake compromises ribosome activity, we measured translation rates in the same strain set. During growth in medium containing 25 μM Mg^{2+}, PstSCAB expression caused a twofold reduction in translation rates relative to control strains (Fig. 7 *B* and *C*). Notably, PstSCAB expression also caused a relative reduction in translation rates during growth in medium containing a 400-fold excess (10 mM) of Mg^{2+} (Fig. 7 *B* and *C*). However, at 10 mM Mg^{2+}, translation rates were approximately twofold higher across all strains (Fig. 7 *B* and *C*). Taken together, these results indicate that the rapid assimilation of too much imported Pi reduces the availability of free cytoplasmic Mg^{2+}, thereby lowering translation efficiency and promoting MgtC expression.

Discussion

We have identified a physiological connection between Pi assimilation and Mg^{2+} homeostasis whereby cells exert tight control over Pi uptake to avoid uncontrollable ATP synthesis and depletion of free cytoplasmic Mg^{2+} (Fig. 1). We establish that the *Salmonella* MgtC protein lowers ATP amounts by inhibiting Pi uptake (Figs. 3 *A–C* and 4*B*), thereby limiting the availability of an ATP precursor rather than interfering with the enzymatic catalysis of ATP-generating reactions per se (Figs. 2 *A–C* and 3 *A–C*). MgtC hinders the activity of a yet unidentified transporter that functions as the main Pi uptake system in *Salmonella* (Fig. 4 *A–F*). This inhibitory activity could take place through a number of different mechanisms. These include 1) a direct physical interaction with the transporter and 2) indirectly through interaction(s) with cellular component(s) that inhibit the Pi transporter activity, synthesis, or degradation. Furthermore, even when cytoplasmic Mg^{2+} is not limiting, excessive Pi uptake leads to increased ATP synthesis, which reduces free cytoplasmic Mg^{2+}, impairing translation and inhibiting growth (Figs. 6 *A–D*, 7 *A–C* and 8).

The Physiological Connection between Pi and Mg^{2+} Homeostasis. The capacity of MgtC to maintain physiological ATP levels during cytoplasmic Mg^{2+} starvation had been so far ascribed to its inhibitory effect on *Salmonella*'s F_1F_o ATP synthase (32). Here, we demonstrate that this inaccurate conclusion resulted from an experimental setting arising from the propagation of *atpB* strains in a poorly fermentable carbon source (Fig. 2 *A–C*). Whereas the function of MgtC in macrophages is associated with the activity of the F_1F_o ATP synthase (32), the specific role of this protein within this biological context is not well understood. Cytoplasmic Mg^{2+} starvation can trigger MgtC expression by impairing the activity of bacterial ribosomes (Fig. 7) (27, 28, 40). However, MgtC promotes *Salmonella* survival irrespective of whether macrophages can restrict the access of bacteria to Mg^{2+} (30, 58, 59). This suggests that a macrophage-induced stress, other than Mg^{2+} starvation, impairs *Salmonella* translation, mimicking a physiological signal experienced during cytoplasmic Mg^{2+} starvation. That is, when inside macrophages, *Salmonella* may "sense" cytoplasmic Mg^{2+} starvation even though Mg^{2+} may not be limiting in the subcellular compartment harboring *Salmonella* (60).

MgtC inhibits Pi uptake independently of all known Pi importers (PitA and PstSCAB) as well as the Pi exporter YjbB.

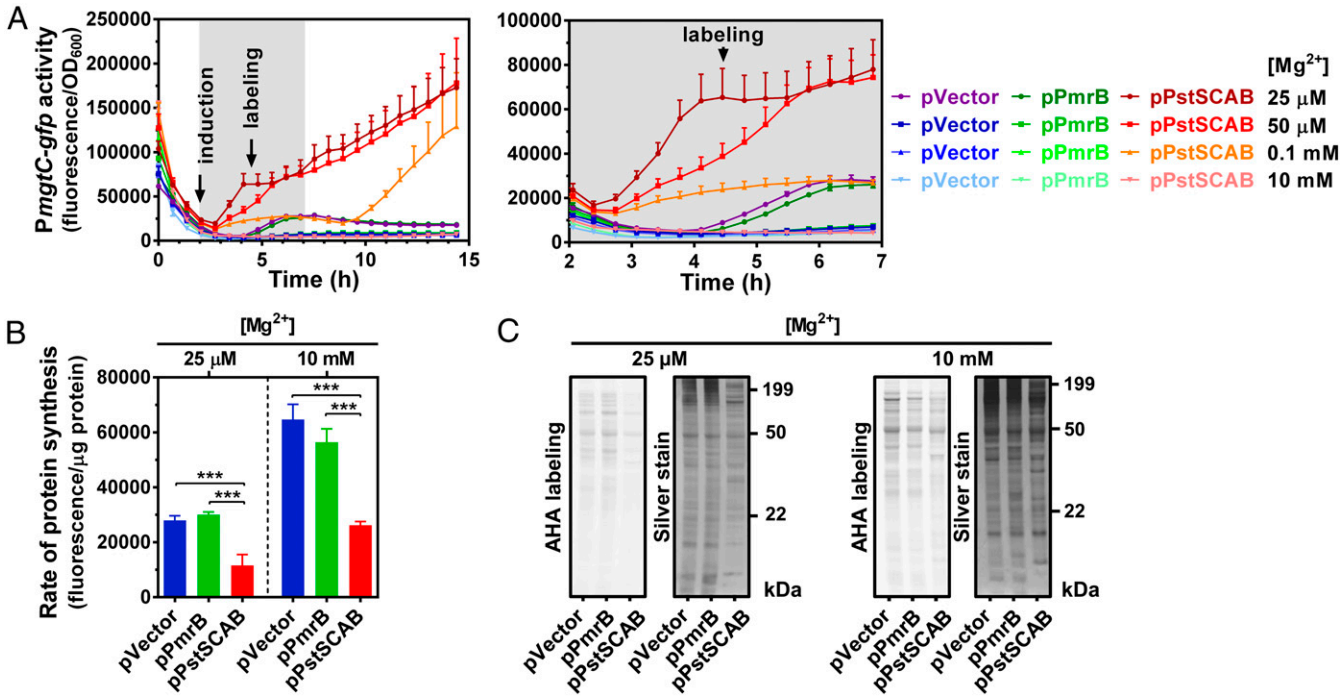

Fig. 7. Effect of PstSCAB expression on *mgtC* transcription and cellular translation rates during growth under conditions of moderate and high Mg^{2+}. (*A*) Fluorescence from wild-type (14028s) *Salmonella* carrying transcriptional reporter p*PmgtC*-GFPc and either pVector (pUHE-21), pPstSCAB (pUHE-PstSCAB), or pPmrB (pUHE-PmrB). Full time course (*Left*) and inset between 2 and 7 h (*Right*) of the experiments are shown. (*B*) Quantification and (*C*) SDS-PAGE analysis of the rate of protein synthesis (L-azidohomoalanine [AHA] labeling) of wild-type (14028s) *Salmonella* carrying either pVector, pPmrB, or pPstSCAB. In all experiments, cells were grown in MOPS medium containing 10 mM K_2HPO_4 and the indicated concentration of $MgCl_2$. For AHA labeling, bacteria were cultured in MOPS medium lacking methionine (see *Materials and Methods*). A total of 250 μM IPTG was added to the cultures following 2 h of growth. AHA was incorporated to the cultures at 4.5 h. Means ± SDs of three independent experiments are shown. Gels are representative of three independent experiments. ***$P < 0.001$, unpaired two-tailed *t* test against pVector.

When heterologously expressed in *E. coli*, MgtC activates the PhoB/PhoR system (*SI Appendix*, Fig. S3). In addition to PstSCAB and PitA, *E. coli* harbors PitB, a Pi importer absent from *Salmonella* (Fig. 4*A*) (1, 51, 61). Notably, *E. coli* strains containing mutations in all of these three Pi transport systems are still able to grow on minimal medium with Pi as the only P source (51, 62). This indicates that *E. coli* encodes an additional Pi transporter(s) that may be targeted by MgtC in *Salmonella*. Given that MgtC sequelogs promote growth in low Mg^{2+} in a large number of distantly related species (34, 63–69), the Pi transporter targeted by MgtC is likely to be widespread in bacteria.

If MgtC inhibits the activity of a single Pi importer, what then prevents Pi uptake by other transport systems? PhoB promotes transcription of the high affinity PstSCAB Pi importer in response to a decrease in cytoplasmic Pi. During the initial stages of cytoplasmic Mg^{2+} starvation, the ribosomal subunits are unable to assemble efficiently (28). This leads to a decrease in translation efficiency and a concomitant reduction in ATP hydrolysis and free cytoplasmic Pi, which triggers *pstSCAB* transcription (17). Whereas MgtC inhibits the main Pi transporter, expression of MgtA and MgtB results in an influx of Mg^{2+} into the cytoplasm (21–26). Both responses restore ribosomal subunit assembly thereby increasing translation efficiency (Fig. 8). ATP consumption during translation (most notably the charging of transfer RNAs and the synthesis of guanosine triphosphate, which is subsequently used by elongation factors) (28) replenishes intracellular Pi, which represses *pstSCAB* transcription by inactivating PhoB/PhoR (17).

The availability of the Pi:Zn^{2+} salt regulates *pitA* transcription (70). In addition, PitA is posttranscriptionally repressed during Mg^{2+} starvation in *E. coli*. This repression is orchestrated by the Mg^{2+}-sensing PhoP/PhoQ two-component system (71), which, in *Salmonella*, activates transcription of *mgtCB* and *mgtA* (21). Because growth in low Mg^{2+} decreases *pitA* mRNA levels in both *Salmonella* and *Yersinia pestis* (72, 73), inhibition of PitA expression appears to be a common feature of the Mg^{2+} starvation response in enteric bacteria. Given that PitA transports M:Pi salts, a reduction in PitA abundance may hinder uptake of other metal cations, such as zinc, that can readily replace scarce Mg^{2+} in enzymatic reactions (74–76). In this context, it is interesting to note that the Pho84 Pi transporter of *Saccharomyces cerevisiae* can promote metal toxicity by importing M:Pi salts (77–80).

If excessive ATP is toxic during cytoplasmic Mg^{2+} starvation, why, then, does MgtC function by hindering Pi uptake and not by directly inhibiting ATP-generating enzyme(s)? Depending on the growth condition, the production of ATP via the oxidation of carbon can occur via several distinct pathways, each involving dozens of enzymes (48). While we can conceive that a single protein may have the capacity to directly inhibit a myriad of distinct enzymes, evolution has likely provided cells with a more parsimonious solution for this problem. Because Pi is an ATP precursor, limitation of Pi uptake enables cells to hinder all ATP generating reactions independently from the metabolic pathway(s) used to oxidize the available carbon source(s) (Figs. 2*B* and 7). Hence, the inhibition of Pi uptake by MgtC allows *Salmonella* to lower ATP synthesis, eliciting a physiological response to a lethal depletion of cytoplasmic Mg^{2+}, whether carbon is being metabolized via classic glycolysis, the Entner–Doudoroff, the Pentose Phosphate, the Tricarboxylic Acid Cycle, or any other energy-generating pathway (Figs. 2*B* and 8).

On the Activation of PhoR by MgtC. Choi et al. reported that MgtC promotes PstSCAB expression and Pi uptake due to PhoB/PhoR activation resulting from a direct physical interaction between the MgtC and PhoR proteins (81). Our data provide independent

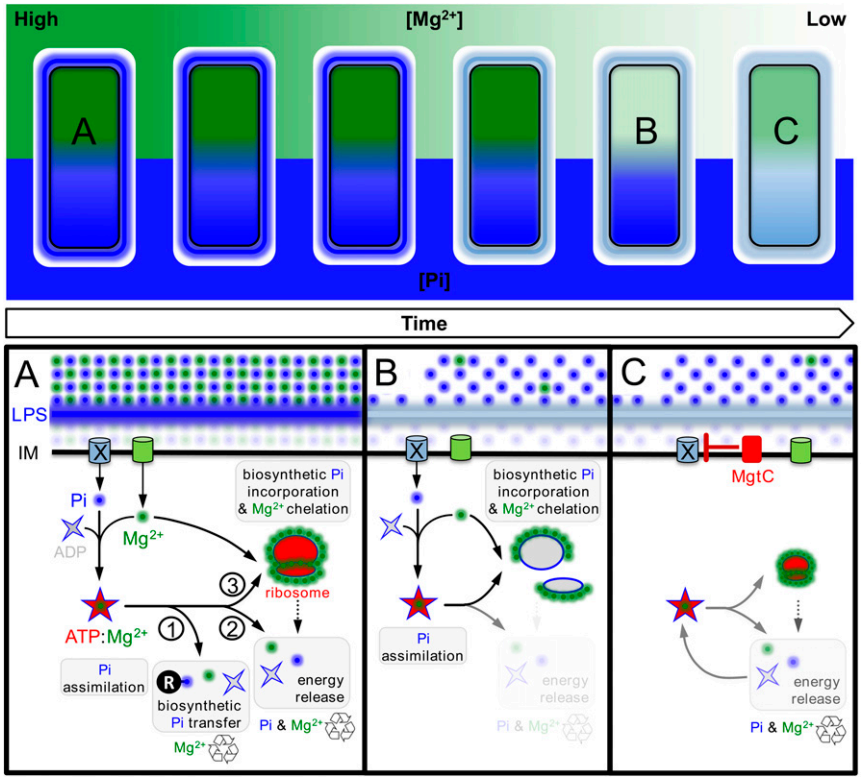

Fig. 8. Model illustrating how limitation of phosphate assimilation maintains cytoplasmic Mg^{2+} homeostasis in *Salmonella enterica*. (*Top*) Overview of the temporal adaptation of *S. enterica* to Mg^{2+} starvation. Mg^{2+} (green) and Pi (blue) concentrations in the environment, lipopolysaccharide (LPS), and cytoplasm are depicted as gradients with dark colors denoting high concentration and light colors representing low concentrations. (*Bottom*) Schematic depicting molecular events and responses underlying the adaptation. (*A*) During homeostasis, Pi is imported into the cytoplasm through dedicated inner membrane (IM) transport systems (X [unknown transporter] and PitA). Cells assimilate imported Pi through the synthesis of ATP, which exists as a salt with positively charged Mg^{2+} (ATP:Mg^{2+}). ATP:Mg^{2+} 1) mediates the transfer of Pi among biological molecules, 2) powers energy-dependent enzymatic reactions, and 3) promotes ribosome biogenesis (1). ATP hydrolysis for the release of energy recycles Pi and Mg^{2+}, whereas the biosynthetic transfer of Pi typically recycles cytoplasmic Mg^{2+}. (*B*) After consuming the Mg^{2+} present in the environment, cells eventually experience a shortage in cytoplasmic Mg^{2+} levels (22, 23, 57). Insufficient cytoplasmic Mg^{2+} impairs ribosomal subunit assembly, lowering translation efficiency (28). This reduces the consumption of ATP by translation reactions and, consequently, decreases the recycling of Mg^{2+} and Pi from ATP:Mg^{2+} (17). (*C*) *Salmonella enterica* expresses the MgtC membrane protein as a homeostatic response to cytoplasmic Mg^{2+} starvation. MgtC inhibits Pi uptake through an unknown transporter (X), thereby preventing assimilation Pi into ATP. As the levels of ATP and ribosomes decrease, free Mg^{2+} ions necessary for core processes such as translation are recovered, increasing the efficiency of protein synthesis and the recycling of Mg^{2+} and Pi from ATP:Mg^{2+}. The density and size of cartoons represent the concentrations of Mg^{2+}, Pi, and ribosomes.

pieces of evidence demonstrating that MgtC actually inhibits Pi uptake, which helps maintain cellular viability during cytoplasmic Mg^{2+} starvation.

First, the proposal that MgtC furthers Pi uptake (81) is incompatible with the fact that Pi is acutely toxic to cells experiencing cytoplasmic Mg^{2+} starvation (Fig. 5 *C* and *D*) and that MgtC is produced in response to cytoplasmic Mg^{2+} starvation (23, 24). Second, during cytoplasmic Mg^{2+} starvation, MgtC expression follows PhoB/PhoR activation and *pstSCAB* transcription, and MgtC production results in inactivation of PhoB/PhoR (*SI Appendix*, Fig. S4 *A* and *B*) (17). Third, this temporal chain of events is supported by a disruption in protein synthesis due to excessive Pi exacerbating cytoplasmic Mg^{2+} starvation and by influx of extracellular Pi via PstSCAB inducing *mgtC* expression (Figs. 6 *A*–*D* and 7 *A*–*C*). And fourth, substitution of the PhoR leucine 421 by an alanine was reported to disrupt PhoR interaction with MgtC, preventing PhoB/PhoR activation in cytoplasmic Mg^{2+} starvation (81). However, wild-type and $phoR^{L421A}$ strains display similar *pstS* transcriptional kinetics in response to ectopic or chromosomal MgtC expression (*SI Appendix*, Fig. S5). Notably, cytoplasmic Mg^{2+} starvation also disrupts translation homeostasis in *E. coli* (28), thereby inducing a shortage in free cytoplasmic Pi and triggering PhoB/PhoR activation (*SI Appendix*, Fig. S6) (17), even though *E. coli* lacks MgtC.

Pi Toxicity and the Control of P Assimilation. Mutations that increase Pi uptake via the PstSCAB transport system inhibit growth in a wide range of bacterial species (1–9). However, the underlying molecular basis for this inhibition has remained elusive. That MgtC promotes growth and viability during cytoplasmic Mg^{2+} starvation (21, 23) by inhibiting Pi uptake (Figs. 3 *A* and *B* and 4*B*) and, consequently, ATP synthesis (Fig. 3*C*) (29) prompted us to examine the physiological basis of Pi toxicity observed in the context of the aforementioned mutations. We established that increased Pi transport via PstSCAB causes a rise in ATP concentrations (Fig. 6*A*). Increased ATP disrupts the pools of free cytoplasmic Mg^{2+} (Fig. 7*A*), thereby inhibiting translation (Fig. 7 *B* and *C*), growth (Fig. 6*B*), and triggering MgtC expression when the Mg^{2+} concentration in the growth medium is sufficiently high to silence its expression (Fig. 7*A*) (22, 23, 27). Our results both establish that the toxic effects of excessive Pi are manifested following its assimilation into ATP and shed light into the underlying causes of Pi toxicity by revealing a logic for cellular control of P assimilation. The rapid synthesis of ATP (Fig. 6 *A*–*C*), and ATP-derived highly charged Pi anions-containing molecules, such as rRNA and poly-Pi (28, 82, 83), depletes the pools of free cytoplasmic Mg^{2+}. Therefore, when biosynthetic precursors are abundant, but Mg^{2+} is

limiting, cells adjust Pi uptake as an effective way to inhibit ATP-generating reactions (Fig. 1).

Materials and Methods

Bacterial Strains, Plasmid Constructs, Primers, and Growth Conditions. The bacterial strains and plasmids used in this study are listed in *SI Appendix*, Table S1, and oligonucleotide sequences are presented in *SI Appendix*, Table S2. Single gene knockouts and deletions were carried out as described (84). Mutations generated via this method were subsequently moved into clean genetic backgrounds via phage P22-mediated transduction as described (85). For chromosomal point mutations, detailed strain construction is described below. Bacterial strains used in recombination and transduction experiments were grown in Luria–Bertani (LB) medium at 30 °C or 37 °C (84–86). When required, the LB medium was supplemented with ampicillin (100 μg/mL), chloramphenicol (20 μg/mL), kanamycin (50 μg/mL), and/or L-arabinose (0.2% wt/vol).

Unless stated otherwise, physiological experiments with bacteria were carried out at 37 °C with shaking at 250 rpm in MOPS medium (87) lacking $CaCl_2$ (to avoid repression of the PhoP/PhoQ system) (88) and supplemented with 0.1% (wt/vol) bacto casamino acids (BD Difco), 25 mM glucose, and the indicated amounts of $MgCl_2$ and K_2HPO_4. Experiments were conducted as follows: After overnight (~16 to 20 h) growth in MOPS medium containing 10 mM $MgCl_2$ and 2 mM K_2HPO_4, cells were washed three times in medium lacking Mg^{2+} and Pi, inoculated (1:100) in fresh medium containing the indicated concentrations of $MgCl_2$ and K_2HPO_4, and propagated for the corresponding amount of time. It should be noted that at a concentration of 0.1% (wt/vol) bacto casamino acids (BD Difco), the medium already contains ~163 μM Pi. During physiological experiments, selection of plasmids was accomplished by the addition of ampicillin at 100 μg/mL (overnight growth) or 30 μg/mL (experimental condition), chloramphenicol at 20 μg/mL (overnight growth) or 10 μg/mL (experimental condition), and/or kanamycin at 50 μg/mL (overnight growth) or 20 μg/mL (experimental condition). Unless specified otherwise, heterologous expression of proteins was achieved by treatment of cultures with 250 μM (pMgtC, pPstSCAB) isopropyl β-D-1-thiogalactopyranoside (IPTG). ATPase expression from pBbB2k-AtpAGD was attained without the addition of the inductor.

Construction of Plasmids Used in This Study. Phusion High-Fidelity DNA Polymerase (New England Biolabs) was used in PCR to amplify DNA inserts. These DNA inserts were cloned into linearized plasmids (17, 27, 89–91) using NEBuilder HiFi DNA Assembly Cloning Kit (New England BioLabs). A detailed construction of plasmids is described in the *SI Appendix*.

Construction of *phoR*^{L421A} Strain. Chromosomal point mutation was generated as described (84, 86). A detailed procedure is described in the *SI Appendix*.

Estimation of Intracellular ATP. Intracellular ATP was estimated as described (17). A detailed description of this method is found in the *SI Appendix*.

Estimation of Intracellular Pi. Total Pi in the samples was estimated from crude cell extracts using the molybdenum blue method (17, 92). A detailed description of this method is found in the *SI Appendix*.

Phosphate Transport Assay. Wild-type (14028s) or *mgtC* (EL4) *Salmonella* were grown in MOPS medium containing 10 μM $MgCl_2$ and 500 μM K_2HPO_4 during 3 h. Wild-type (14028s) or Δ3Pi (RB39) cells harboring either pVector or pMgtC were grown in MOPS containing 250 μM $MgCl_2$ and 500 μM K_2HPO_4 until OD_{600} ~0.2, at which point, MgtC expression was induced for 15 min with the addition of 750 μM IPTG. To assay the transport of Pi, 20 μCi of radioactive Pi solution (10 μL from a 2 mCi $K_2H^{32}PO_4$ at a concentration of 2 mM $K_2H^{32}PO_4$, PerkinElmer catalog number NEX055) was added to 1 mL cell suspension. At the indicated time points, 50 μL of each sample was submitted to rapid filtration through 0.45 μm mixed cellulose ester membrane filters (Whatman) with an applied vacuum. The filters were washed three times with 1 mL PBS buffer and subsequently soaked in 5 mL scintillation fluid (Research Products International). The amount of radioactivity taken up by the cells was determined with a scintillation counter (Triathler multilabel tester, HIDEX) using the ^{32}P-window and by counting each vial for 20 s. Radioactive counts per minute were normalized by protein content using a Rapid Gold BCA Protein Assay Kit (Pierce). ^{32}Pi uptake of each sample was normalized against the corresponding control in each independent experiment.

Monitoring Bacterial Growth and Gene Expression via Fluorescence. Bacterial growth and fluorescence measurements were performed using SpectraMax i3x plate reader (Molecular Devices). The detailed protocols are described in the *SI Appendix*.

L-azidohomoalanine Protein Labeling and Quantification. In vivo labeling of proteins and estimation of translation rates were performed as described (26), with minor modifications highlighted in the *SI Appendix*.

Image Acquisition, Analysis, and Manipulation. Plates, gel, and membrane images were acquired using an Amersham Imager 600 (GE Healthcare Life Sciences). ImageJ software (93) was used to crop the edges and adjust the brightness and contrast of the images. These modifications were simultaneously performed across the entire set images to be shown.

Data Availability. All study data are included in the article and/or *SI Appendix*.

ACKNOWLEDGMENTS. M.H.P. is supported by Grant AI148774 from the NIH and funds from The Pennsylvania State University College of Medicine. E.A.G. is supported by Grant AI49561 from the NIH.

1. B. L. Wanner, "Phosphorus assimilation and control of the phosphate regulon" in *Escherichia Coli and Salmonella: Cellular and Molecular Biology*, F. C. Neidhardt *et al*., Eds. (American Society for Microbiology, ed. 2, 1996), pp. 1357–1381.
2. D. C. Webb, H. Rosenberg, G. B. Cox, Mutational analysis of the *Escherichia coli* phosphate-specific transport system, a member of the traffic ATPase (or ABC) family of membrane transporters. A role for proline residues in transmembrane helices. *J. Biol. Chem.* **267**, 24661–24668 (1992).
3. P. M. Steed, B. L. Wanner, Use of the *rep* technique for allele replacement to construct mutants with deletions of the *pstSCAB-phoU* operon: Evidence of a new role for the PhoU protein in the phosphate regulon. *J. Bacteriol.* **175**, 6797–6809 (1993).
4. T. Morohoshi *et al*., Accumulation of inorganic polyphosphate in *phoU* mutants of *Escherichia coli* and *Synechocystis* sp. strain PCC6803. *Appl. Environ. Microbiol.* **68**, 4107–4110 (2002).
5. C. D. Rice, J. E. Pollard, Z. T. Lewis, W. R. McCleary, Employment of a promoter-swapping technique shows that PhoU modulates the activity of the $PstSCAB_2$ ABC transporter in *Escherichia coli*. *Appl. Environ. Microbiol.* **75**, 573–582 (2009).
6. L. G. de Almeida, J. H. Ortiz, R. P. Schneider, B. Spira, *phoU* inactivation in *Pseudomonas aeruginosa* enhances accumulation of ppGpp and polyphosphate. *Appl. Environ. Microbiol.* **81**, 3006–3015 (2015).
7. E. A. Lubin, J. T. Henry, A. Fiebig, S. Crosson, M. T. Laub, Identification of the PhoB regulon and role of PhoU in the phosphate starvation response of *Caulobacter crescentus*. *J. Bacteriol.* **198**, 187–200 (2015).
8. J. J. Zheng, D. Sinha, K. J. Wayne, M. E. Winkler, Physiological roles of the dual phosphate transporter systems in low and high phosphate conditions and in capsule maintenance of *Streptococcus pneumoniae* D39. *Front. Cell. Infect. Microbiol.* **6**, 63 (2016).
9. G. C. diCenzo, H. Sharthiya, A. Nanda, M. Zamani, T. M. Finan, PhoU allows rapid adaptation to high phosphate concentrations by modulating PstSCAB transport rate in *Sinorhizobium meliloti*. *J. Bacteriol.* **199**, 1–20 (2017).
10. M. E. Maguire, J. A. Cowan, Magnesium chemistry and biochemistry. *Biometals* **15**, 203–210 (2002).
11. A. C. Storer, A. Cornish-Bowden, Concentration of MgATP2- and other ions in solution. Calculation of the true concentrations of species present in mixtures of associating ions. *Biochem. J.* **159**, 1–5 (1976).
12. D. A. Schneider, T. Gaal, R. L. Gourse, NTP-sensing by rRNA promoters in *Escherichia coli* is direct. *Proc. Natl. Acad. Sci. U.S.A.* **99**, 8602–8607 (2002).
13. H. D. Murray, D. A. Schneider, R. L. Gourse, Control of rRNA expression by small molecules is dynamic and nonredundant. *Mol. Cell* **12**, 125–134 (2003).
14. M. H. Pontes, A. Sevostyanova, E. A. Groisman, When too much ATP is bad for protein synthesis. *J. Mol. Biol.* **427**, 2586–2594 (2015).
15. D. J. Klein, P. B. Moore, T. A. Steitz, The contribution of metal ions to the structural stability of the large ribosomal subunit. *RNA* **10**, 1366–1379 (2004).
16. R. F. Gesteland, Unfolding of *Escherichia coli* ribosomes by removal of magnesium. *J. Mol. Biol.* **18**, 356–371 (1966).
17. M. H. Pontes, E. A. Groisman, Protein synthesis controls phosphate homeostasis. *Genes Dev.* **32**, 79–92 (2018).
18. J. F. Gillooly *et al*., The metabolic basis of whole-organism RNA and phosphorus content. *Proc. Natl. Acad. Sci. U.S.A.* **102**, 11923–11927 (2005).
19. J. J. Elser *et al*., Growth rate-stoichiometry couplings in diverse biota. *Ecol. Lett.* **6**, 936–943 (2003).
20. H. Bremer, P. P. Dennis, Modulation of chemical composition and other parameters of the cell at different exponential growth rates. *Ecosal Plus*, **3** (2008).
21. F. C. Soncini, E. García Véscovi, F. Solomon, E. A. Groisman, Molecular basis of the magnesium deprivation response in *Salmonella* typhimurium: Identification of PhoP-regulated genes. *J. Bacteriol.* **178**, 5092–5099 (1996).
22. M. J. Cromie, Y. Shi, T. Latifi, E. A. Groisman, An RNA sensor for intracellular Mg^{2+}. *Cell* **125**, 71–84 (2006).

23. S. V. Spinelli, L. B. Pontel, E. García Véscovi, F. C. Soncini, Regulation of magnesium homeostasis in *Salmonella*: Mg^{2+} targets the *mgtA* transcript for degradation by RNase E. *FEMS Microbiol. Lett.* **280**, 226–234 (2008).
24. E. A. Groisman *et al*., Bacterial Mg^{2+} homeostasis, transport, and virulence. *Annu. Rev. Genet.* **47**, 625–646 (2013).
25. M. D. Snavely, C. G. Miller, M. E. Maguire, The *mgtB* Mg^{2+} transport locus of *Salmonella* typhimurium encodes a P-type ATPase. *J. Biol. Chem.* **266**, 815–823 (1991).
26. T. Tao, M. D. Snavely, S. G. Farr, M. E. Maguire, Magnesium transport in *Salmonella* typhimurium: *mgtA* encodes a P-type ATPase and is regulated by Mg^{2+} in a manner similar to that of the *mgtB* P-type ATPase. *J. Bacteriol.* **177**, 2654–2662 (1995).
27. E. J. Lee, E. A. Groisman, Control of a *Salmonella* virulence locus by an ATP-sensing leader messenger RNA. *Nature* **486**, 271–275 (2012).
28. M. H. Pontes, J. Yeom, E. A. Groisman, Reducing ribosome biosynthesis promotes translation during low Mg^{2+}stress. *Mol. Cell* **64**, 480–492 (2016).
29. M. H. Pontes, E. J. Lee, J. Choi, E. A. Groisman, *Salmonella* promotes virulence by repressing cellulose production. *Proc. Natl. Acad. Sci. U.S.A.* **112**, 5183–5188 (2015).
30. A. B. Blanc-Potard, E. A. Groisman, The *Salmonella selC* locus contains a pathogenicity island mediating intramacrophage survival. *EMBO J.* **16**, 5376–5385 (1997).
31. S. Eriksson, S. Lucchini, A. Thompson, M. Rhen, J. C. Hinton, Unravelling the biology of macrophage infection by gene expression profiling of intracellular *Salmonella enterica*. *Mol. Microbiol.* **47**, 103–118 (2003).
32. E. J. Lee, M. H. Pontes, E. A. Groisman, A bacterial virulence protein promotes pathogenicity by inhibiting the bacterium's own F_1F_o ATP synthase. *Cell* **154**, 146–156 (2013).
33. D. Okuno, R. Iino, H. Noji, Rotation and structure of FoF1-ATP synthase. *J. Biochem.* **149**, 655–664 (2011).
34. C. Rang *et al*., Dual role of the MgtC virulence factor in host and non-host environments. *Mol. Microbiol.* **63**, 605–622 (2007).
35. K. Aung *et al*., *pho2*, a phosphate overaccumulator, is caused by a nonsense mutation in a microRNA399 target gene. *Plant Physiol.* **141**, 1000–1011 (2006).
36. T. T. Nguyen *et al*., Mitochondrial oxidative stress mediates high-phosphate-induced secretory defects and apoptosis in insulin-secreting cells. *Am. J. Physiol. Endocrinol. Metab.* **308**, E933–E941 (2015).
37. M. Luan *et al*., Vacuolar phosphate transporters contribute to systemic phosphate homeostasis vital for reproductive development in *Arabidopsis*. *Plant Physiol.* **179**, 640–655 (2019).
38. M. S. Razzaque, Phosphate toxicity: New insights into an old problem. *Clin. Sci. (Lond.)* **120**, 91–97 (2011).
39. M. Park, D. Nam, D.-H. Kweon, D. Shin, ATP reduction by MgtC and Mg^{2+} homeostasis by MgtA and MgtB enables *Salmonella* to accumulate RpoS upon low cytoplasmic Mg^{2+} stress. *Mol. Microbiol.* **110**, 283–295 (2018).
40. M. Park, H. Kim, D. Nam, D.-H. Kweon, D. Shin, The *mgtCBR* mRNA leader secures growth of *Salmonella* in both host and non-host environments. *Front. Microbiol.* **10**, 2831 (2019).
41. A. E. Senior, The proton-translocating ATPase of *Escherichia coli*. *Annu. Rev. Biophys. Biophys. Chem.* **19**, 7–41 (1990).
42. F. M. Harold, P. C. Maloney, "Energy transduction by ion currents" in *Escherichia Coli and Salmonella: Cellular and Molecular Biology*, F. C. Neidhardt *et al*., Eds. (American Society for Microbiology, ed. 2, 1996), pp. 283–306.
43. J. D. Butlin, G. B. Cox, F. Gibson, Oxidative phosphorylation in *Escherichia coli* K-12: The genetic and biochemical characterisations of a strain carrying a mutation in the *uncB* gene. *Biochim. Biophys. Acta* **292**, 366–375 (1973).
44. A. Murarka, Y. Dharmadi, S. S. Yazdani, R. Gonzalez, Fermentative utilization of glycerol by *Escherichia coli* and its implications for the production of fuels and chemicals. *Appl. Environ. Microbiol.* **74**, 1124–1135 (2008).
45. K. Richter, J. Gescher, Accelerated glycerol fermentation in *Escherichia coli* using methanogenic formate consumption. *Bioresour. Technol.* **162**, 389–391 (2014).
46. A. G. Marr, Growth rate of *Escherichia coli*. *Microbiol. Rev.* **55**, 316–333 (1991).
47. J. B. Russell, G. M. Cook, Energetics of bacterial growth: Balance of anabolic and catabolic reactions. *Microbiol. Rev.* **59**, 48–62 (1995).
48. M. T. Madigan, J. M. Martinko, K. S. Bender, D. H. Buckley, D. A. Stahl, "Microbial metabolism" in *Brock Biology of Microorganisms* (Pearson, ed. 14, 2015), pp. 73–105.
49. H. Rosenberg, R. G. Gerdes, K. Chegwidden, Two systems for the uptake of phosphate in *Escherichia coli*. *J. Bacteriol.* **131**, 505–511 (1977).
50. H. W. van Veen, T. Abee, G. J. Kortstee, W. N. Konings, A. J. Zehnder, Translocation of metal phosphate via the phosphate inorganic transport system of *Escherichia coli*. *Biochemistry* **33**, 1766–1770 (1994).
51. R. M. Harris, D. C. Webb, S. M. Howitt, G. B. Cox, Characterization of PitA and PitB from *Escherichia coli*. *J. Bacteriol.* **183**, 5008–5014 (2001).
52. G. B. Cox, D. Webb, H. Rosenberg, Specific amino acid residues in both the PstB and PstC proteins are required for phosphate transport by the *Escherichia coli* Pst system. *J. Bacteriol.* **171**, 1531–1534 (1989).
53. K. Motomura *et al*., Overproduction of YjbB reduces the level of polyphosphate in *Escherichia coli*: A hypothetical role of YjbB in phosphate export and polyphosphate accumulation. *FEMS Microbiol. Lett.* **320**, 25–32 (2011).
54. S. G. Gardner, K. D. Johns, R. Tanner, W. R. McCleary, The PhoU protein from *Escherichia coli* interacts with PhoR, PstB, and metals to form a phosphate-signaling complex at the membrane. *J. Bacteriol.* **196**, 1741–1752 (2014).
55. B. L. Wanner, Novel regulatory mutants of the phosphate regulon in *Escherichia coli* K-12. *J. Mol. Biol.* **191**, 39–58 (1986).
56. A. Sevostyanova, E. A. Groisman, An RNA motif advances transcription by preventing Rho-dependent termination. *Proc. Natl. Acad. Sci. U.S.A.* **112**, E6835–E6843 (2015).
57. M. J. Cromie, E. A. Groisman, Promoter and riboswitch control of the Mg^{2+} transporter MgtA from *Salmonella enterica*. *J. Bacteriol.* **192**, 604–607 (2010).
58. O. Cunrath, D. Bumann, Host resistance factor SLC11A1 restricts *Salmonella* growth through magnesium deprivation. *Science* **366**, 995–999 (2019).
59. J. Yeom, Y. Shao, E. A. Groisman, Small proteins regulate *Salmonella* survival inside macrophages by controlling degradation of a magnesium transporter. *Proc. Natl. Acad. Sci. U.S.A.* **117**, 20235–20243 (2020).
60. A. B. Blanc-Potard, E. A. Groisman, How pathogens feel and overcome magnesium limitation when in host tissues. *Trends Microbiol.* **29**, 98–106 (2021).
61. S. M. Hoffer, P. Schoondermark, H. W. van Veen, J. Tommassen, Activation by gene amplification of *pitB*, encoding a third phosphate transporter of *Escherichia coli* K-12. *J. Bacteriol.* **183**, 4659–4663 (2001).
62. S. M. Hoffer, J. Tommassen, The phosphate-binding protein of *Escherichia coli* is not essential for P(i)-regulated expression of the pho regulon. *J. Bacteriol.* **183**, 5768–5771 (2001).
63. N. Buchmeier *et al*., A parallel intraphagosomal survival strategy shared by *mycobacterium tuberculosis* and *Salmonella enterica*. *Mol. Microbiol.* **35**, 1375–1382 (2000).
64. J. P. Lavigne, D. O'callaghan, A. B. Blanc-Potard, Requirement of MgtC for *Brucella suis* intramacrophage growth: A potential mechanism shared by *Salmonella enterica* and *Mycobacterium tuberculosis* for adaptation to a low-Mg^{2+} environment. *Infect. Immun.* **73**, 3160–3163 (2005).
65. K. E. Maloney, M. A. Valvano, The *mgtC* gene of *Burkholderia cenocepacia* is required for growth under magnesium limitation conditions and intracellular survival in macrophages. *Infect. Immun.* **74**, 5477–5486 (2006).
66. C. Belon, L. Gannoun-Zaki, G. Lutfalla, L. Kremer, A. B. Blanc-Potard, *Mycobacterium marinum* MgtC plays a role in phagocytosis but is dispensable for intracellular multiplication. *PLoS One* **9**, e116052 (2014).
67. C. Belon *et al*., A macrophage subversion factor is shared by intracellular and extracellular pathogens. *PLoS Pathog.* **11**, e1004969 (2015).
68. V. Le Moigne *et al*., MgtC as a host-induced factor and vaccine candidate against *Mycobacterium abscessus* infection. *Infect. Immun.* **84**, 2895–2903 (2016).
69. J. H. Cafiero, Y. A. Lamberti, K. Surmann, B. Vecerek, M. E. Rodriguez, A *Bordetella pertussis* MgtC homolog plays a role in the intracellular survival. *PLoS One* **13**, e0203204 (2018).
70. R. J. Jackson *et al*., Expression of the PitA phosphate/metal transporter of *Escherichia coli* is responsive to zinc and inorganic phosphate levels. *FEMS Microbiol. Lett.* **289**, 219–224 (2008).
71. X. Yin *et al*., The small protein MgtS and small RNA MgrR modulate the PitA phosphate symporter to boost intracellular magnesium levels. *Mol. Microbiol.* **111**, 131–144 (2019).
72. S. Srikumar *et al*., RNA-seq brings new insights to the intra-macrophage transcriptome of *Salmonella* Typhimurium. *PLoS Pathog.* **11**, e1005262 (2015).
73. J. C. Perez *et al*., Evolution of a bacterial regulon controlling virulence and Mg^{2+} homeostasis. *PLoS Genet.* **5**, e1000428 (2009).
74. S. J. Beard *et al*., Evidence for the transport of zinc(II) ions via the pit inorganic phosphate transport system in *Escherichia coli*. *FEMS Microbiol. Lett.* **184**, 231–235 (2000).
75. T. Dudev, C. Lim, Principles governing Mg, Ca, and Zn binding and selectivity in proteins. *Chem. Rev.* **103**, 773–788 (2003).
76. A. W. Foster, D. Osman, N. J. Robinson, Metal preferences and metallation. *J. Biol. Chem.* **289**, 28095–28103 (2014).
77. L. T. Jensen, M. Ajua-Alemanji, V. C. Culotta, The *Saccharomyces cerevisiae* high affinity phosphate transporter encoded by PHO84 also functions in manganese homeostasis. *J. Biol. Chem.* **278**, 42036–42040 (2003).
78. L. Rosenfeld *et al*., The effect of phosphate accumulation on metal ion homeostasis in *Saccharomyces cerevisiae*. *J. Biol. Inorg. Chem.* **15**, 1051–1062 (2010).
79. L. Rosenfeld, V. C. Culotta, Phosphate disruption and metal toxicity in *Saccharomyces cerevisiae*: Effects of RAD23 and the histone chaperone HPC2. *Biochem. Biophys. Res. Commun.* **418**, 414–419 (2012).
80. A. M. Ofiteru *et al*., Overexpression of the PHO84 gene causes heavy metal accumulation and induces Ire1p-dependent unfolded protein response in *Saccharomyces cerevisiae* cells. *Appl. Microbiol. Biotechnol.* **94**, 425–435 (2012).
81. S. Choi *et al*., The *Salmonella* virulence protein MgtC promotes phosphate uptake inside macrophages. *Nat. Commun.* **10**, 3326 (2019).
82. A. K. Rudat, A. Pokhrel, T. J. Green, M. J. Gray, Mutations in *Escherichia coli* polyphosphate kinase that lead to dramatically increased *in vivo* polyphosphate levels. *J. Bacteriol.* **200**, 10.1128/JB.00697-17 (2018).
83. Y. Li *et al*., The composition and implications of polyphosphate-metal in enhanced biological phosphorus removal systems. *Environ. Sci. Technol.* **53**, 1536–1544 (2019).
84. S. Datta, N. Costantino, D. L. Court, A set of recombineering plasmids for gram-negative bacteria. *Gene* **379**, 109–115 (2006).
85. R. Davis, D. Bolstein, J. Roth, *Advanced Bacterial Genetics* (Cold Spring Harbor Lab Press, Cold Spring Harbor, NY, 1980).
86. V. Khetrapal *et al*., A set of powerful negative selection systems for unmodified Enterobacteriaceae. *Nucleic Acids Res.* **43**, e83 (2015).
87. F. C. Neidhardt, P. L. Bloch, D. F. Smith, Culture medium for enterobacteria. *J. Bacteriol.* **119**, 736–747 (1974).
88. E. García Véscovi, F. C. Soncini, E. A. Groisman, Mg^{2+} as an extracellular signal: Environmental regulation of *Salmonella* virulence. *Cell* **84**, 165–174 (1996).
89. F. C. Soncini, E. García Véscov, E. A. Groisman, Transcriptional autoregulation of the *Salmonella* typhimurium *phoPQ* operon. *J. Bacteriol.* **177**, 4364–4371 (1995).
90. T. S. Lee *et al*., BglBrick vectors and datasheets: A synthetic biology platform for gene expression. *J. Biol. Eng.* **5**, 12 (2011).
91. A. C. Chang, S. N. Cohen, Construction and characterization of amplifiable multicopy DNA cloning vehicles derived from the P15A cryptic miniplasmid. *J. Bacteriol.* **134**, 1141–1156 (1978).
92. S. Kanno *et al*., Performance and limitations of phosphate quantification: Guidelines for plant biologists. *Plant Cell Physiol.* **57**, 690–706 (2016).
93. C. A. Schneider, W. S. Rasband, K. W. Eliceiri, NIH image to ImageJ: 25 years of image analysis. *Nat. Methods* **9**, 671–675 (2012).